Characterization of primary fersmite from the Mount Brussilof magnesite deposit, southeastern British Columbia, Canada

George J. Simandl[1, a, 2], Joseph A. Petrus[3], Matthew I. Leybourne[4], Suzanne Paradis[5], and Carlee Akam[1]

[1] British Columbia Geological Survey, Ministry of Energy, Mines and Petroleum Resources, Victoria, BC, V8W 9N3
[2] School of Earth and Ocean Sciences, University of Victoria, BC, V8P 5C2
[3] Mineral Exploration Research Centre, Harquail School of Earth Sciences, Laurentian University, Sudbury, ON, P3E 2C6
[4] Queen's Facility for Isotope Research, Department of Geological Sciences and Geological Engineering, Kingston, ON, K7L 3N6
[5] Geological Survey of Canada, Natural Resources Canada, Sidney, BC, V8L 4B2
[a] corresponding author: George.Simandl@gov.bc.ca

Abstract

Fersmite ($[Ca,Ce,Na][Nb,Ta,Ti]_2[O,OH,F]_6$) is a complex mineral, occurring commonly as a strongly metamict alteration product of pre-existing niobate minerals in carbonatites, alkaline and peralkaline intrusions, and rare element pegmatites. Most well-documented primary fersmite localities in Europe are 'alpine cleft', also referred to as 'alpine fissure', occurrences. At Mount Brussilof in southeastern British Columbia, fersmite occurs as an accessory mineral on sparry dolomite crosscutting and lining cavities in sparry magnesite. The fersmite forms brittle, black, submetallic to vitreous lustre, acicular to platy crystals up to 2 cm long. It also forms smaller, commonly fractured or broken, crystals (<3 mm) enclosed by sparry dolomite. Sparry dolomite is commonly associated with Mississippi Valley-type Zn-Pb deposits, both globally and within southeastern British Columbia. Electron microprobe and laser ablation inductively coupled plasma mass spectrometry mapping indicate that the Mount Brussilof fersmite is rich in Nb, Th, and heavy REE, and poor in Ta. Individual fersmite crystals are strongly zoned in terms of Na, Ti, Fe, Y, all REE, Ta, Pb isotopes (^{204}Pb, ^{206}Pb, ^{207}Pb, and ^{208}Pb), Th, and U, suggesting that the chemical composition of hydrothermal or carbohydrothermal fluids from which fersmite precipitated evolved with time. The textural and chemical properties of the Mount Brussilof fersmite differ from those found in carbonatite- and pegmatite-related deposits. The zonation, non-metamict appearance, and enrichment in Nb relative to Ta of the Mount Brussilof fersmite may help to distinguish fersmite formed in similar settings (alpine-clefts) from fersmite formed in pegmatites, peralkaline intrusions, carbonatites, and other geological environments, and enhance its use as a direct indicator mineral.

Keywords: Primary fersmite, chemical zoning, Mount Brussilof, magnesite, sparry dolomite, dolomitization, Mississippi Valley-type deposits

1. Introduction

The Mount Brussilof sparry magnesite deposit, currently the only magnesite-producing mine in Canada, is 40 km northeast of Invermere in the Rocky Mountain Foreland Belt of the southern Canadian Cordillera (Fig. 1). The spatial relationship between the Mount Brussilof deposit and Mississippi Valley-type (MVT) deposits such as Shag, Hawk Creek, Kicking Horse, and Monarch, and their position along the Kicking Horse rim (Fig. 2) was highlighted by Aitken and McIlreath (1984), Simandl et al. (1992), and Paradis and Simandl (2017, 2018). At the Mount Brussilof deposit, sparry dolomite zones cut sparry magnesite (Simandl and Hancock, 1991). Fersmite ($[Ca,Ce,Na][Nb,Ta,Ti]_2[O,OH,F]_6$) is hosted by the sparry dolomite or by sugary dolomite enclosed in the sparry dolomite.

Globally, fersmite is the third most important Nb-ore mineral after pyrochlore supergroup minerals and columbite-tantalite solid solution series minerals (Mackay and Simandl, 2014; Simandl et al., 2018). However, the Mount Brussilof fersmite occurrence is too small to be of economic interest as a source of niobium. Nevertheless, it may have metallogenic implications. Assuming there is only one generation of sparry dolomite in southeastern British Columbia, or if fersmite is hosted by the youngest generation of sparry dolomite, then the circulation of Nb-bearing fluids along the faults related to the Cathedral escarpment post-dates MVT Zn-Pb, REE-Ba-fluorite, and magnesite mineralization in the region.

The objectives of this study are to: 1) describe the Mount Brussilof fersmite occurrence; 2) define the relationships between fersmite, sparry dolomite, and sparry magnesite; 3) characterize the compositional zoning observed in fersmite and present the most likely hypothesis regarding its origin; and 4) compare the physical and chemical properties of the Mount Brussilof fersmite to those of fersmite from carbonatite- and pegmatite-related deposits, furthering the value of fersmite as a direct indicator mineral.

113

Geological Fieldwork 2018, British Columbia Ministry of Energy, Mines and Petroleum Resources, British Columbia Geological Survey Paper 2019-01

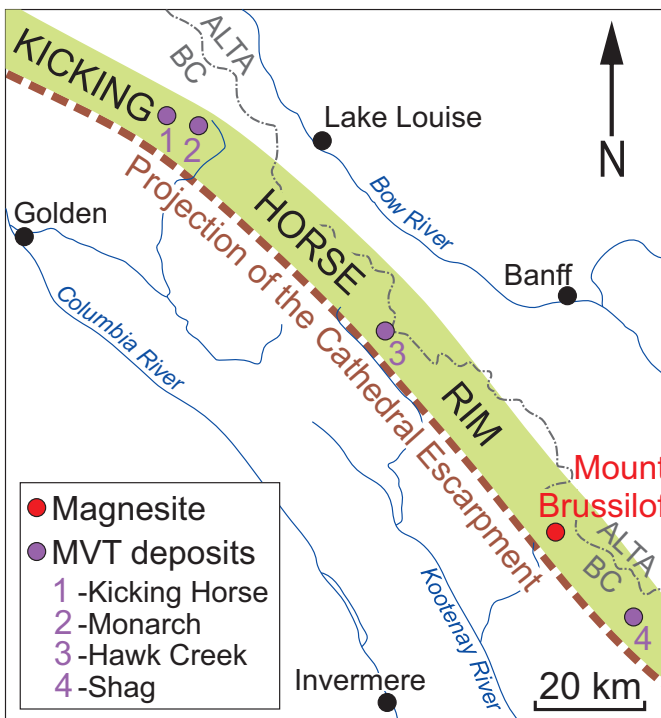**Fig. 1.** Location of the Mount Brussilof magnesite mine.

Fig. 2. Kicking Horse Rim bounded on the west by the projection of the Cathedral escarpment (Aitkin, 1971). Mount Brussilof magnesite mine and selected MVT deposits. 1- Kicking Horse mine; 2- Monarch mine; 3- Hawk Creek prospect; and 4- Shag prospect. All are northeast of the Cathedral Escarpment and hosted by carbonate rocks deposited in shallow-marine environments (modified from Simandl et al., 1992).

2. Geological setting

The Mount Brussilof magnesite deposit is along the Kicking Horse rim (Fig. 2), a north-northwest trending paleo-topographic high defined by Aitken (1971, 1989). The southwestern edge of the Kicking Horse rim coincides with the Cathedral escarpment, a Middle Cambrian reef margin (Aitken and McIlreath, 1984, 1990; Fritz, 1990). The rocks northeast of the escarpment (Fig. 2), including the Cathedral Formation (Middle Cambrian) that hosts the Mount Brussilof magnesite deposit, were deposited in a shallow-marine environment, whereas rocks of the Chancellor Group that outcrop southwest of the escarpment are off-reef, deeper water deposits (Aitken, 1978; Simandl and Hancock, 1991; Simandl et al., 1992). In the Mount Brussilof area, the projection of the Cathedral escarpment coincides with the 'faulted facies change' mapped by Leech (1966) and with the Mitchell River fault on the most recent regional map (McMechan and Leech, 2011). The stratigraphy of the Mount Brussilof mine area and geology of the deposit is summarized by Simandl and Hancock (1991). The relationships between dolomite, sparry magnesite, sparry dolomite, and Zn-Pb MVT mineralization is covered by Paradis and Simandl (2018). Fersmite post-dates sparry dolomite, which cross cuts sparry magnesite. The sparry magnesite is hosted by the Cathedral Formation (Middle Cambrian).

3. Fersmite

Aeschynite-group minerals and euxenite-group minerals, which include fersmite ($[Ca,Ce,Na][Nb,Ta,Ti]_2[O,OH,F]_6$), are orthorhombic. The groups share the formula AB_2O_6. The A-site is commonly occupied by Y, REE, Ca, Na, U, and Th, and the B-site contains Ti, Nb, and Ta. Despite similarities in occupancies of the A- and B-sites of these mineral groups, LREE are preferentially incorporated into the aeschynite-group minerals, whereas Y and HREE are preferentially incorporated into the euxenite group (Ercit, 2005; Škoda and Novák, 2007).

Globally, fersmite occurs mostly as a strongly metamict alteration product of pre-existing niobate minerals in carbonatites (e.g., Aley Carbonatite in British Columbia, Mäder, 1987; Chakhmouradian et al., 2015) and alkaline and peralkaline intrusions (e.g., Ilímaussaq complex in South Greenland; Karup-Møller et al., 2010). Rare element pegmatites (e.g., Prašivá in Slovakia, Uher et al., 1998; Wodgina in Western Australia, Sweetapple and Lumpkin, 2011; and pegmatites of the Třebíč Pluton in the Czech Republic, Škoda and Novák, 2007) are also known to contain secondary or late fersmite. Lumpkin and Ewing (1992) explain the mineral stability relationship between fersmite-ferrocolumbite ($FeNb_2O_6$) and pyrochlore ($[Na,Ca]_2Nb_2O_6[OH,F]$) in the Na-Ca-Fe-Nb-O-H system (which approximates magmatic-hydrothermal systems) in terms of Na^+, Ca^{2+}, and Fe^{2+} activities.

Primary fersmite is less common. It occurs mainly as prismatic crystals that are predominantly tabular, blade-shaped, or acicular. Crystals are black, dark brown, or lemon-yellow to yellow-brown, and their luster varies from resinous to subvitreous or submetallic. Many dark-colored crystals are nearly opaque, fluoresce yellow-green to bluish-green under shortwave and longwave ultraviolet light, and have a pale blue cathodoluminescence (Anthony et al., 2017). Well-documented localities containing prismatic fersmite crystals correspond to

114

Geological Fieldwork 2018, British Columbia Ministry of Energy, Mines and Petroleum Resources, British Columbia Geological Survey Paper 2019-01

'alpine cleft' occurrences (also referred to as 'alpine fissures'), defined by Niggli et al. (1940) as open joints, vugs and other cavities partially filled with well crystallized (commonly euhedral) minerals formed during metamorphism and uplift of mountain belts. The origin of fluids carrying Nb and REE from which primary fersmite crystallizes has not been clearly identified in published studies.

At the Mount Brussilof magnesite deposit, fersmite is an erratically distributed trace mineral. The fersmite-bearing zone, now mined out, was approximately 10 m long, irregular, and porous. It consisted of sugary dolomite and sparry dolomite that cuts sparry magnesite. The zone was exposed a few metres from a pyrite stockwork in the sparry magnesite. The Mount Brussilof fersmite forms brittle, black, acicular to platy crystals up to 2 cm long with a submetallic to vitreous lustre that line cavities in sparry dolomite. In some cavities, fersmite occurs with euhedral quartz (Fig. 3). Fersmite also occurs as smaller crystals enclosed in dolomite (Fig. 4). The Mount Brussilof fersmite does not replace earlier Nb-bearing minerals and, resembling 'alpine cleft' varieties that have been described from sites in Europe, may be the first primary fersmite recognized in British Columbia. The samples selected for detailed geochemical studies consist of black, striated, prismatic fersmite crystals about 0.5 to 2.0 mm long.

4. Analytical methods

Four fersmite-bearing polished thin sections were produced from samples collected at the Mount Brussilof deposit, and analyzed (MB-16-01, MB-16-02A, MB-16-02B, and MB-16-02C). Black, striated, grains suspected to be Nb-rutile or fersmite were selected for electron microprobe (EMP), laser ablation inductively coupled plasma mass spectrometry (LA-ICP-MS), and wavelength-dispersive spectroscopy (WDS). Independently, a concentrate of the black striated grains
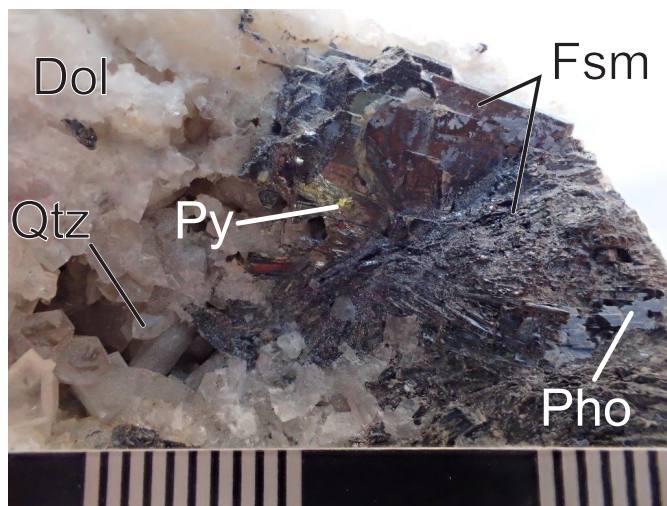

Fig. 3. Coarse fersmite crystals (Fsm) lining a cavity in sparry dolomite and locally intergrown with late sugary dolomite (Dol). Quartz (Qtz), pyrite (Py), and phosphate (Pho) are also present. Coarsest fersmite lining the cavity has apparent brownish reflections along cleavages. Mount Brussilof mine, scale in cm.
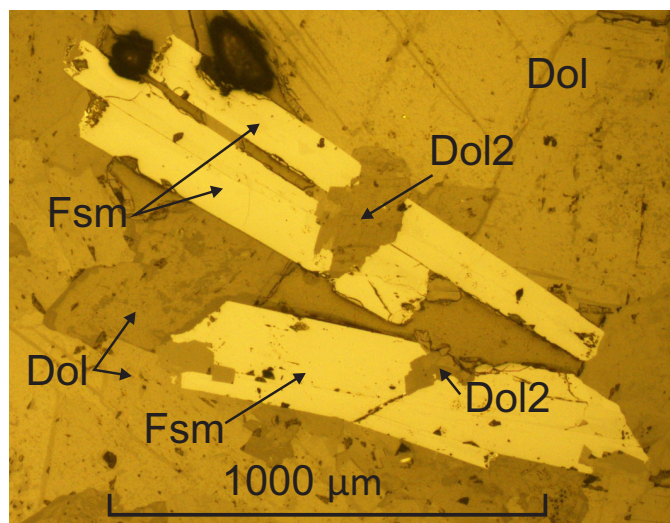

Fig. 4. Photomicrograph of zoned fersmite (Fsm) crystals enclosed in sparry dolomite (Dol), reflected light. Late dolomite (Dol2) fills fractures in fersmite. Mount Brussilof mine.

intended for X-ray powder diffraction (XRD) analysis was produced by crushing the rock with a hammer and steel plate, and hand-picking under a binocular microscope. The results of XRD, EMP, and LA-ICP-MS analyses are essential to chemically characterize the Mount Brussilof fersmite.

4.1. X-ray powder diffraction

A hand-picked concentrate of niobate minerals was analyzed at the University of British Columbia. The concentrate was ground under ethanol with a corundum mortar and pestle and dispersed onto a zero-diffraction quartz plate using ethanol. Continuous-scan XRD data were collected over a range 3-80° 2q with Co Kα radiation on a Bruker D8 Focus Bragg-Brentano diffractometer equipped with a Fe-monochromator foil, 0.6 mm (0.3°) divergence slit, incident- and diffracted-beam Soller slits and a LynxEye detector. The long fine-focus Co X-ray tube was operated at 35 kV and 40 mA, using a take-off angle of 6°. The XRD of the concentrate was needed to confirm the identity of the Ca-niobate, because fersmite has a similar Nb/Ca value to vigezzite (an aeschynite-group mineral with a generalized formulae [Ca,Ce][Nb,Ta,Ti]$_2$O$_6$).

4.2. Electron microprobe analyses

Selected fersmite grains were analyzed by EMP using a Cameca SX50 at the Central Analytical Facility, Laurentian University. Operating conditions were 20 kV and 20 nA using a focused beam and WDS acquisition and the correction procedure described by Pouchou and Pichoir (1984) was applied. Standards used were APS25 (F), Albite (Na), Wake Diopside (Ca), CaTiO$_3$ (Ti), YPO$_4$, (Y), MnNb$_2$O$_6$ (Nb), CePO$_4$ (Ce) and LiTaO$_3$ (Ta). Count times were 15 s (F, Y, Ce, Ta) and 30 s (Na, Ca, Ti, Nb).

115

Geological Fieldwork 2018, British Columbia Ministry of Energy, Mines and Petroleum Resources, British Columbia Geological Survey Paper 2019-01

4.3. Laser Ablation Inductively Coupled Plasma Mass Spectrometry

The trace element contents of fersmite were determined by LA-ICP-MS at Laurentian University, Ontario. The measurements were made in situ by ablating the grains with a Resonetics (now Australian Scientific Instruments) RESOlution M-50 laser ablation system employing a Coherent CompexPRO ArF 193 nm wavelength, 20 ns pulse duration laser and a Laurin Technic two-volume laser ablation cell (Müller et al., 2009). Ablation took place in ultra-pure He flowing at 650 ml/min. The He and ablation aerosol were combined with N_2 (6 ml/min) and Ar (750 ml/min) immediately outside the ablation cell and transferred to the torch of the ICP-MS by approximately 3 meters of tubing. The ablated material was analyzed by a Thermo X-Series II ICP-MS operating with a forward power of 1450 W. Prior to each session, the ICP-MS was tuned while ablating NIST612 to maximize sensitivity and minimize oxide production (<0.5%) while maintaining Th/U ~1. Different isotopes were analyzed in each session as the preceding measurements showed significant trace element variation. Dwell times during analysis were 5-10 ms for major and trace elements, and 20-40 ms for U-Th-Pb (^{206}Pb:30, ^{207}Pb:40, ^{208}Pb:20, ^{232}Th:20, ^{238}U:30). Spot data were collected using a beam diameter of 48 μm, repetition rate of 6 Hz, and fluence of 5 J/cm².

Because the chemistry of the initial spot analyses appeared to be complex, several grains were laser mapped to reveal the elemental relationships in more detail. The maps were acquired by ablating a series of parallel and adjacent traverses over the regions of interest. To improve the spatial resolution, a smaller spot size of 14 μm was used with a scan speed of 7 μm/s and repetition rate of 8 Hz.

Calibration was carried out using certified reference materials NIST610, NIST612, and BHVO2G, each of which were analyzed before, after, and periodically during each analytical session. The data were processed using Iolite version 3.4 (Paton et al., 2011). The trace element contents were calculated using the "TraceElements_IS" data reduction scheme of Iolite with NIST610 as the external standard and Nb (53.28 wt.%; mean of WDS data) as the internal standard.

5. Results

Exploratory EMP analysis determined that the grains of unknown, black mineral were either fersmite or vigezzite ([Ca,Ce][Nb,Ta,Ti]$_2$O$_6$). The XRD analyses confirmed conclusively that all black, striated grains with sub-vitreous luster previously analyzed by EMP and LA-ICP-MS are fersmite (Fig. 5).

Electron microprobe analyses of grains from samples MB-16-01 and MB-16-02 are listed in Table 1. A statistical summary of LA-ICP-MS analyses of REE in grains from these samples is presented in Table 2, and chondrite-normalized REE patterns for sample MB-16-02 first quartile, median, and third quartile based on 189 spot analyses are displayed in Figure 6. A series of compositional maps were produced to link the variations

in chemical composition to their position within individual grains (e.g., Fig. 7). The Mount Brussilof fersmite is Nb-rich (Table 1), averages 53.3 wt.% Nb, and has low Ta contents (below the limit of quantification by EMP, 180 ppm) relative to fersmite from other geological environments. Compositional maps of fersmite crystals (e.g., Fig. 7) show well-developed zonation in terms of Na, Ti, Fe, Y, all REE, Ta, Pb isotopes (^{204}Pb, ^{206}Pb, ^{207}Pb, and ^{208}Pb), Th, and U.

6. Discussion

Fersmite from the Mount Brussilof deposit is interpreted as primary based on its prismatic crystal form and textural habit (Figs. 3, 4). This is in contrast with other fersmite occurrences in British Columbia where fersmite is an alteration product of previously formed niobates. Euhedral fersmite crystals formed in open spaces on sparry dolomite (Fig. 3) but are locally transected by a later-stage dolomite (Dol 2 in Fig. 4). Thus fersmite crystallized between episodes of dolomite growth. Because the sparry dolomite crosscuts the magnesite ore, the fersmite also post-dates magnesite.

Coarse-grained, white sparry dolomite, referred to as 'saddle' dolomite in the exploration industry, forms by interaction of high temperature hydrothermal fluids with precursor carbonates and is commonly used as an exploration guide for MVT Zn-Pb mineralization (Leach et al., 2005; Paradis et al., 2007). Sparry magnesite may have a similar origin. For the Mount Brussilof sparry magnesite, one possible mechanism considers that carbonate minerals convert to magnesite under moderate fluid temperature conditions (<200°C), assuming a one mole concentration, and a one to one mole ratio of Ca^{2+} to Mg^{2+} equivalent of seawater (Rosenberg et al., 1967; Simandl and Hancock, 1991). An alternative mechanism involves the conversion of Mg-rich magnesite precursors precipitated in an evaporitic environment into magnesite (Simandl and Hancock, 1998).

The timing of sparry dolomitization in the Rocky Mountain Foreland belt of the Canadian Cordillera and the Western Canada Sedimentary Basin remains contentious. There is evidence for at least two periods of sparry dolomitization coinciding with tectonic activity (Al-Aasm et al., 2000; Al-Aasm, 2003); the first corresponds to the Late Devonian-Early Mississippian 'Antler Orogeny' (Root, 2001), and the second to the Late Cretaceous-Eocene fold and thrust belt (Laramide Orogeny; Symons et al., 1999). Studies by Al-Aasm (2003) and Mrad (2016) conducted in the northwestern portion of the Western Canada Sedimentary Basin suggest that distinction between different pulses of dolomitization may be possible based on, for example, δ^{18}O and ^{87}Sr/^{86}Sr values of sparry dolomite, and fluid salinity. A comparable study in the Rocky Mountain Foreland belt in southeastern British Columbia (Nesbitt and Prochaska, 1998) containing additional information on solute chemistry of fluid inclusions (Na/Br, Cl/Br, and I/Br values) in dolomite and magnesite suggests that formation of sparry dolomite, magnesite, talc, and MVT deposits hosted by Middle Cambrian carbonate rocks preceded the Laramide orogeny. This, in
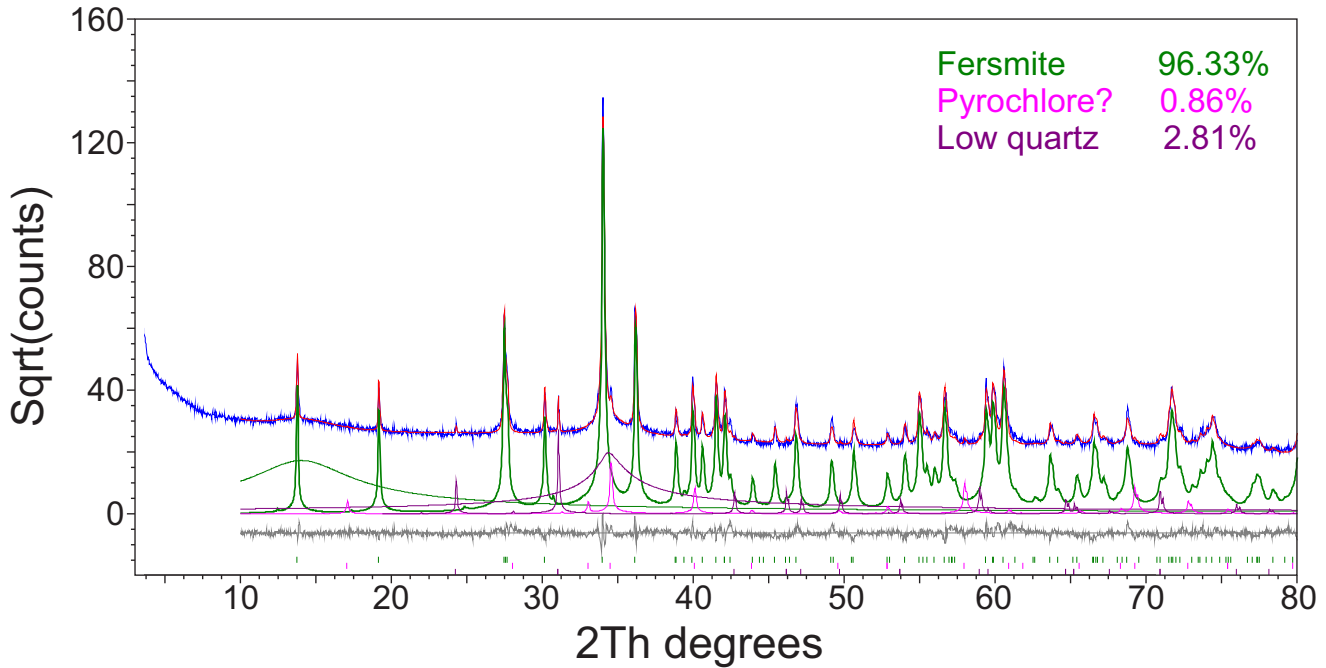
116

Geological Fieldwork 2018, British Columbia Ministry of Energy, Mines and Petroleum Resources, British Columbia Geological Survey Paper 2019-01

Fig. 5. Rietveld refinement plot of fersmite from sample MB16-01. Blue line - observed intensity at each step; red line - calculated pattern; solid grey line below - difference between observed and calculated intensities; vertical bars - positions of all Bragg reflections. Individual diffraction patterns of fersmite in green, of possible pyrochlore in pink, and of low quartz in purple.
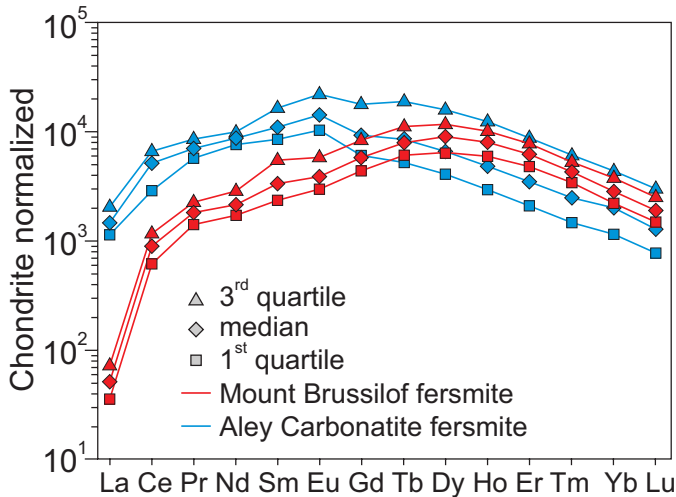

Fig. 6. Chondrite-normalized median, and upper and lower quartile REE distribution for fersmite from Mount Brussilof sample MB-16-02 (based on 189 spot analyses) and for fersmite from the Aley carbonatite (Chakhmouradian et al., 2015). Chondrite values are from McDonough and Sun (1995).

combination with the fluid flow model of Yao and Demicco (1995, 1997) and ongoing research of Paradis and Simandl (2017; 2018) will be components of a modern metallogenic synthesis of southeastern British Columbia. Fersmite, a Nb- and REE- bearing mineral, is hosted by sparry dolomite, which post-dates sparry magnesite. It also coexists with or pre-dates sugary dolomite, both of which post-date the sparry dolomite. These relationships may provide a key constraint on the timing of sparry dolomitization and MVT mineralization along the Kicking Horse rim, and possibly elsewhere. It may be relevant to interpreting the genesis of the sparry dolomite-associated Rock Canyon Creek REE-F deposit 73 km south-southeast from Mount Brussilof.

6.1. Chemical composition of fersmite

In Figure 8 we compare the weight proportions of Ca, Nb, and Ta x 10 of fersmite compositions from the Mount Brussilof magnesite deposit to fersmite compositions from Aley carbonatite in northeastern British Columbia (Chakhmouradian et al., 2015); Upper Fir carbonatite in east-central British Columbia (Chudy, 2013); Sunsas Belt placer deposit, Bolivia (Alfonso et al., 2015); Prasiva Pegmatites, Slovakia (Uher et al., 1998); Skoddefjellet Pegmatite, Norway (Prsek et al., 2010); Alpe Rosso Pegmatite, Italy (Guastoni et al., 2008); and Baveno Pegmatite, Italy (Aurisicchio et al., 2001). It also compares these weight proportions to the Huron Claim Pegmatite, Manitoba (average of two analyses) and Himalaya Pegmatite and King's Mountain Pegmatite (Foote Mine), USA (Foord and Mrose, 1978). The Ta content of fersmite from the Aley and Upper Fir carbonatites is probably representative of most fersmite-bearing carbonatites. Five of the values from the Aley carbonatite form a tight cluster and two plot within or near the cluster formed by fersmite from the Upper Fir carbonatite. The Upper Fir fersmite is expected to have relatively high Ta content relative to fersmite from most carbonatites because the Ta content of Upper Fir niobate minerals (pyrochlore and columbite) is relatively high (Simandl et al., 2002). Tantalum content of fersmite from pegmatites is more variable than that

117

Geological Fieldwork 2018, British Columbia Ministry of Energy, Mines and Petroleum Resources, British Columbia Geological Survey Paper 2019-01
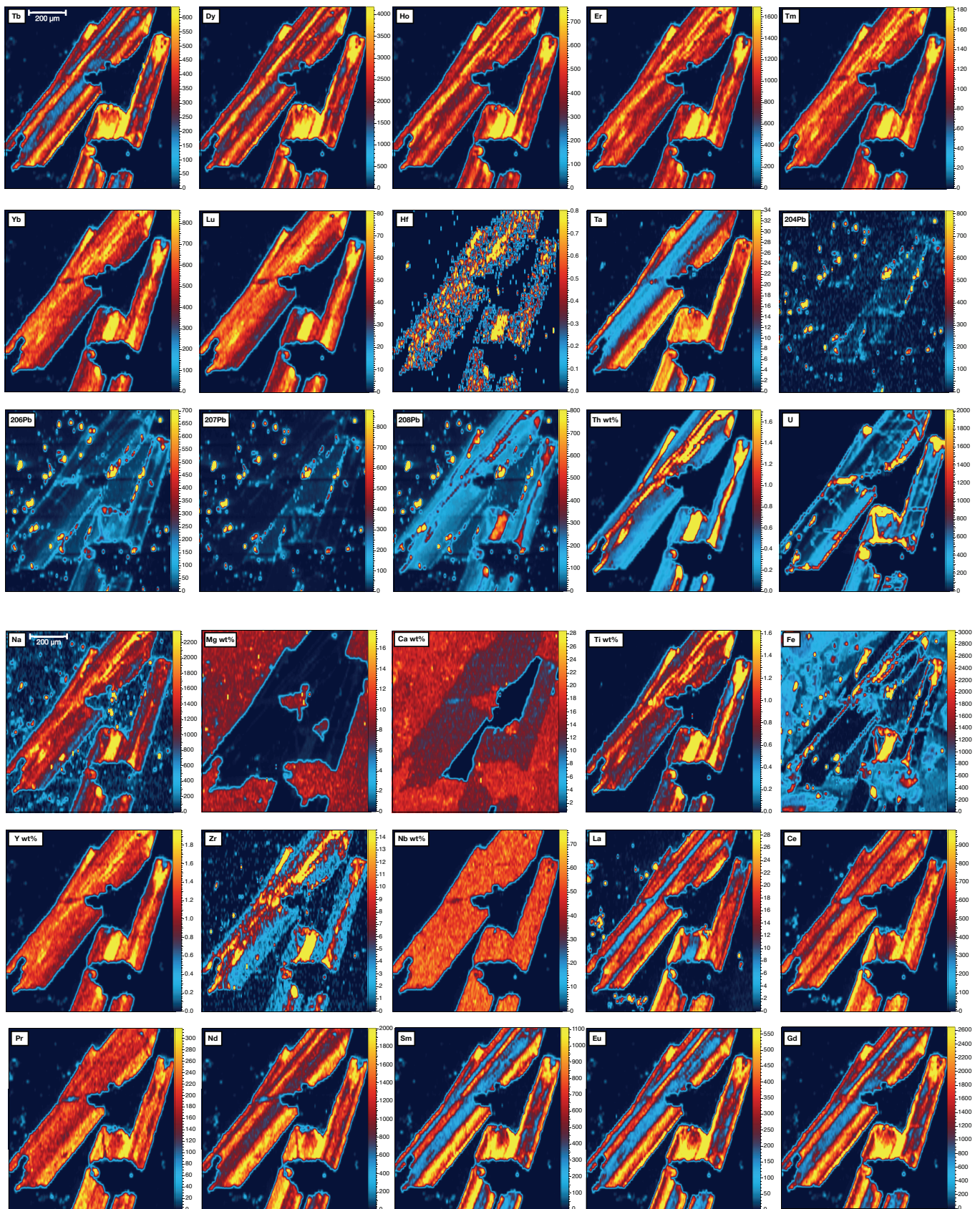
Fig. 7. Compositional LA-ICP-MS map of fersmite grains from sample MB-16-02A. The color scales are linear with minimums and maximums defined by the median ±3 standard deviations. Note that this implies that some pixels are below and above the color extremes. Concentrations are in ppm unless noted otherwise. Scale of 200 µm visible on the Na and Tb maps applies to all maps.

118

Geological Fieldwork 2018, British Columbia Ministry of Energy, Mines and Petroleum Resources, British Columbia Geological Survey Paper 2019-01

Fig. 8. Ca-Nb-Ta x 10 compositions in weight proportions of fersmite from the Mount Brussilof magnesite mine (red), carbonatite (blue), pegmatite (pink), and placer (green) deposits.

of fersmite from carbonatites, and extends closer to the Ta x 10 apex (Fig. 8). This ternary diagram is relevant to use of fersmite as a direct indicator mineral and for targeting specific Nb-Ta deposit types (see section 6.3).

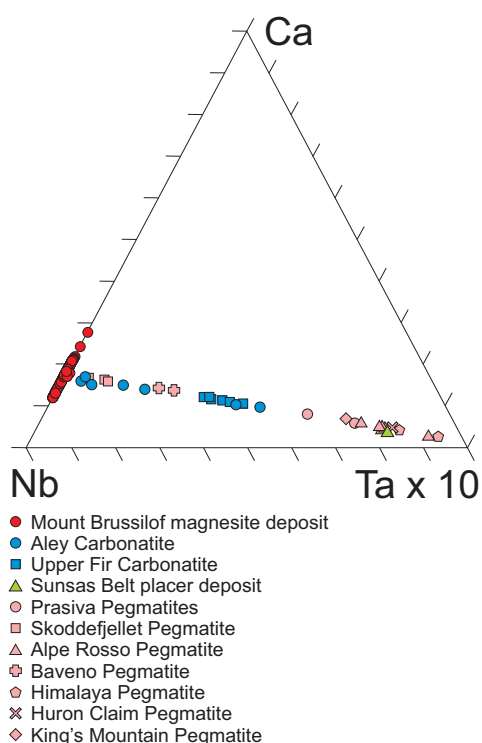Fersmite is a euxenite group mineral; consequently, it preferentially incorporates Y and HREE in its crystal structure relative to LREE (Ercit, 2005; Škoda and Novák, 2007). The chondrite-normalized REE pattern of the Mount Brussilof fersmite is smooth and convex-upward and similar to fersmite in the Aley carbonatite, albeit with lower LREE (Fig. 6). The maximum of the Mount Brussilof fersmite chondrite-normalized REE pattern is shifted towards heavier REE relative to the Aley carbonatite fersmite pattern, possibly indicating that the mineralizing system at Mount Brussilof had a higher HREE:LREE ratio than that at Aley. This observation may be important for mineral deposit targeting based on direct indicator minerals (see section 6.3) because carbonatites typically have a higher LREE:HREE ratio than other lithologies (e.g., Simandl and Paradis, 2018).

It is possible that the atypical (Nb-rich) composition of the Mount Brussilof fersmite reflects the composition of fluids from which it precipitated. Experimental studies of fluoride-rich systems suggest that as fluids interact with the country rocks and their composition evolves, the mobility of Nb remains higher than that of Ta at pH of 2, and up to a temperature of 250°C, over a wide range of HF concentrations (Timofeev et

Table 1. Electron microprobe analyses (wt.%) of fersmite in polished thin sections MB-16-01 and MB-16-02.

Sample	Na_2O	CaO	TiO_2	Y_2O_3	Nb_2O_5	Ce_2O_3	Ta_2O_5	F	Total
MB-02-1	0.07	15.82	0.91	0.76	79.50	0.00	0.00	0.04	97.10
MB-02-2	0.30	12.01	3.50	2.04	70.73	0.05	0.00	0.09	88.72
MB-02-3	0.11	15.43	1.48	0.87	78.89	0.09	0.04	0.00	96.91
MB-02-4	0.10	15.70	1.05	0.63	79.02	0.09	0.00	0.02	96.62
MB-02-5	0.08	15.77	1.09	0.69	78.74	0.07	0.00	0.00	96.43
MB-02-6	0.07	16.22	0.80	0.27	80.09	0.06	0.00	0.00	97.50
MB-02-7	0.10	15.70	0.86	0.60	79.69	0.05	0.01	0.00	97.01
MB-02-8	0.18	14.72	2.52	1.27	76.46	0.07	0.00	0.04	95.25
MB-02-9	0.14	15.52	1.11	0.85	78.87	0.10	0.00	0.01	96.61
MB-02-10	0.33	12.43	2.86	1.52	71.73	0.02	0.00	0.00	88.88
MB-01-1	0.06	16.48	0.84	0.00	78.09	0.30	0.00	0.06	95.83
MB-01-2	0.17	15.84	0.75	0.05	77.45	0.15	0.00	0.12	94.53
MB-01-3	0.11	15.14	2.47	0.32	73.56	0.20	0.05	0.09	91.95
MB-01-4	0.14	16.07	0.51	0.00	77.83	0.20	0.00	0.04	94.79
MB-01-5	0.32	9.55	3.59	0.00	68.03	0.63	0.00	0.00	82.13
MB-01-6	0.41	14.37	1.66	0.18	74.07	0.09	0.00	0.02	90.79
MB-01-7	0.14	15.89	0.97	0.14	76.60	0.10	0.00	0.07	93.91
MB-01-8	0.18	15.86	0.73	0.22	76.86	0.21	0.00	0.01	94.07
MB-01-9	0.14	14.68	3.17	0.65	72.24	0.07	0.00	0.02	90.96
MB-01-10	0.07	16.28	1.22	0.00	75.83	0.41	0.00	0.00	93.82

119

Geological Fieldwork 2018, British Columbia Ministry of Energy, Mines and Petroleum Resources, British Columbia Geological Survey Paper 2019-01

Table 2. Statistical summary of trace element composition (ppm) of fersmite for polished thin sections MB-16-01, MB-16-02A, MB-16-02B, and MB-16-02C.

Sample	MB-16-01	n=30				MB-16-02A	n=61			
Element	Minimum	1st Quartile	Median	3rd Quartile	Maximum	Minimum	1st Quartile	Median	3rd Quartile	Maximum
Na	157.90	618.00	1185.00	1684.00	3333.00	744.00	1052.00	1155.00	1477.00	3022.00
Mg						12.90	180.00	420.00	1971.00	16400.00
Si										
Ca	102700.00	115250.00	119200.00	121250.00	127200.00	98900.00	108300.00	111800.00	113100.00	133900.00
Ti	3594.00	5087.50	8080.00	13132.50	23220.00	5840.00	7930.00	10180.00	14730.00	28610.00
Cr						1.82	2.46	3.09	3.90	4.70
Fe						6.40	85.68	402.00	1138.75	3027.00
Y						10700.00	14260.00	15800.00	17960.00	26390.00
Zr						1.65	5.11	7.24	11.34	26.22
La						6.14	13.64	17.35	20.60	25.54
Ce	773.00	1021.75	1271.50	1670.00	2512.00	471.00	586.00	660.00	754.00	845.00
Pr						176.50	211.70	230.70	247.90	333.10
Nd						913.00	1163.00	1380.00	1802.00	2649.00
Sm	591.00	1688.00	2252.00	3359.50	8110.00	287.90	481.00	640.00	990.00	1563.00
Eu						136.20	227.60	323.20	477.00	798.00
Gd						797.00	1232.00	1789.00	2396.00	4120.00
Tb						208.60	307.00	438.00	554.00	870.00
Dy						1783.00	2411.00	2920.00	3454.00	5960.00
Ho						398.90	499.00	561.00	701.00	1099.00
Er						943.00	1186.00	1332.00	1643.00	2452.00
Tm						93.70	129.30	139.90	170.60	280.20
Yb	48.90	141.95	255.30	377.98	621.00	419.00	604.00	679.00	801.00	1204.00
Lu						37.95	59.54	67.50	76.30	105.60
Hf						0.16	0.30	0.39	0.55	1.29
Ta	2.91	5.26	10.16	14.83	20.48	5.89	11.10	18.19	27.50	44.55
W										
^{204}Pb	1.04	1.43	1.70	2.47	9.50	1.00	2.65	4.40	9.40	29.50
^{206}Pb	8.44	17.70	49.65	90.70	453.00	5.39	14.09	25.00	50.10	128.80
^{207}Pb	1.74	3.10	4.55	6.46	25.20	1.79	3.18	4.76	11.60	29.00
^{208}Pb	57.00	87.65	169.90	259.35	507.00	45.70	97.80	165.30	252.40	820.00
Bi										
Th	3998.00	6079.75	11025.00	17627.50	35880.00	3020.00	6510.00	10750.00	16480.00	52100.00
U	75.80	154.50	607.00	999.00	4739.00	47.90	140.00	274.30	622.00	1171.00

al., 2017). Under such conditions, both Nb and Ta are expected to precipitate rapidly upon removal of fluoride from an acidic brine (Timofeev et al., 2015, 2017). Fluorite was not observed close to the Mount Brussilof fersmite occurrence, suggesting that this fersmite may have formed from distal, relatively low concentration fluids (some F may have been incorporated by the crystal structure of mica found locally in the magnesite mine area). Because the fersmite occurrence is small, it is also possible that fersmite precipitated due to fluid mixing. More work is required to clarify the origin of the Mount Brussilof fersmite occurrence.

6.2. Compositional maps of individual fersmite crystals

The systematic zonation shown on the compositional maps of fersmite (Fig. 7) explains the relatively high degree of variability in the spot data, and indirectly confirms the internal consistency of the trace element data (Table 2). This zonation suggests a mineralizing system that evolved during fersmite crystallization. In combination with the non-metamict

appearance of the Mount Brussilof fersmite, the zonation helps distinguish the Mount Brussilof and possibly 'alpine cleft' fersmite from that formed in pegmatites, peralkaline intrusions, carbonatites, and other geological environments.

6.3. Fersmite as direct indicator mineral

The physical and chemical properties of primary fersmite make it a useful direct indicator mineral for carbonatites and related deposits. Indicator minerals are defined by McClenaghan (2005, p. 233) as "mineral species that, when appearing as transported grains in clastic sediments, indicate the presence in bedrock of a specific type of mineralization, hydrothermal alteration or lithology. Their physical and chemical characteristics, including a relatively high density, facilitate their preservation and identification and allow them to be readily recovered at the parts per billion level from sample media such as till, stream sediments or soil producing large exploration targets". An indicator mineral that contains pathfinder elements characteristic of a targeted deposit in

Table 2. Continued.

Sample	MB-16-02B	n=46				MB-16-02C	n=82			
Element	Minimum	1st Quartile	Median	3rd Quartile	Maximum	Minimum	1st Quartile	Median	3rd Quartile	Maximum
Na	652.00	805.25	1033.00	1425.25	2236.00	248.80	422.25	561.00	683.50	2281.00
Mg	12.00	50.70	305.50	1216.25	4600.00	14.30	32.90	128.50	799.75	31900.00
Si						1600.00	2150.00	2500.00	2800.00	4900.00
Ca	76200.00	96125.00	100600.00	105575.00	203000.00	71400.00	82825.00	84950.00	89400.00	142000.00
Ti	3400.00	4647.50	5271.00	6692.50	9240.00	2200.00	3580.00	4352.50	6002.50	12400.00
Cr	1.33	1.54	1.65	1.94	2.80	1.86	2.10	2.42	3.00	6.20
Fe	6.20	87.60	256.50	667.00	3158.00	4.50	15.68	65.25	514.25	2690.00
Y	9070.00	10900.00	13385.00	15095.00	21420.00	10560.00	13235.00	14015.00	15322.50	23270.00
Zr	2.28	4.09	7.14	10.28	17.95	0.91	3.19	4.03	5.88	21.70
La	4.58	14.38	15.76	18.40	48.60	1.41	6.56	8.59	10.47	22.20
Ce	343.00	516.00	547.70	604.50	813.00	117.90	286.50	334.60	404.05	580.00
Pr	140.30	160.88	178.50	203.53	238.50	81.70	101.83	122.00	141.53	205.90
Nd	619.00	899.50	1032.00	1336.50	1656.00	382.00	619.50	758.00	930.25	1467.00
Sm	187.20	342.75	450.50	776.50	1001.00	139.30	260.00	354.50	451.50	796.00
Eu	90.40	163.93	222.65	366.15	476.00	68.60	128.50	174.70	224.78	449.00
Gd	495.00	884.75	1162.00	1664.00	2278.00	373.00	674.75	926.50	1189.25	2350.00
Tb	128.40	228.95	295.60	399.00	619.00	97.00	171.45	227.00	303.68	1200.00
Dy	1104.00	1866.00	2171.00	2650.25	4250.00	775.00	1228.00	1559.50	2289.50	8570.00
Ho	252.30	374.48	420.35	504.25	887.00	171.10	254.45	323.40	394.75	1614.00
Er	660.00	835.25	972.00	1167.50	1834.00	434.00	598.25	758.00	892.75	2060.00
Tm	73.30	89.00	106.20	125.53	179.50	46.90	65.18	81.45	96.78	164.10
Yb	322.00	418.00	501.50	611.75	772.00	201.30	313.48	383.50	440.00	697.00
Lu	29.68	42.20	51.70	60.93	73.80	19.04	31.69	36.59	42.15	68.60
Hf	1.30	2.04	2.35	2.78	4.34	0.19	0.45	0.66	0.87	1.86
Ta	4.49	6.85	11.05	19.35	23.54	1.98	3.54	5.22	9.78	16.55
W						140.40	754.00	1064.50	1276.00	1806.00
204Pb	1.23	2.18	2.60	3.15	11.00	2.60	3.50	4.20	5.20	15.50
206Pb	3.03	8.98	20.44	27.69	76.30	2.05	4.47	8.05	15.93	74.60
207Pb	1.16	1.96	2.41	3.03	13.79	0.85	1.42	1.85	3.00	17.80
208Pb	42.40	60.15	126.75	234.50	533.00	20.93	56.13	72.40	125.28	478.00
Bi						0.03	0.04	0.04	0.05	0.09
Th	4020.00	6177.50	11120.00	20045.00	53100.00	4440.00	9275.00	11220.00	19385.00	62100.00
U	9.26	101.50	239.45	319.28	614.00	3.88	39.85	91.75	179.48	1270.00

concentrations detectable by commonly applied analytical methods such as portable XRF or traditional, laboratory-based analytical methods is referred to as a 'direct' indicator mineral (Simandl et al., 2017).

The direct indicator mineral concept involves using traditional geochemical methods to identify sediment samples with anomalous concentrations of pathfinder elements, followed by analysis of anomalous samples by Quantitative Evaluation of Materials by Scanning Electron Microscopy, or QEMSCAN®(Simandl et al., 2017). This two-step approach provides the equivalent of geochemical and indicator mineral surveys without expensive and time-consuming traditional indicator mineral surveys involving hand-picking. Fersmite, as well as pyrochlore supergroup and columbite-tantalite series minerals, REE-fluorocarbonates, and monazite, were used as direct indicator minerals in orientation surveys targeting carbonatites and related deposits in British Columbia (Mackay et al., 2016; Simandl et al., 2018). Fersmite from carbonatites and related deposits is Nb-rich, whereas fersmite from pegmatites may have significantly higher Ta content (Fig. 8). It remains unclear if the composition of fersmite from

Mount Brusilof is representative of 'alpine-cleft' style fersmite occurrences. More work is required to determine which the case is; nevertheless, our summary (Fig. 8) is the first step in developing a fersmite discrimination diagram for mineral exploration and deposit targeting.

7. Summary

The Mount Brussilof fersmite is characterized by strongly zoned euhedral crystals growing on the walls of cavities, or enclosed in a sugary dolomite matrix within sparry dolomite zones that crosscut magnesite ore. It post-dates sparry dolomitization and formation of magnesite ore. The Mount Brussilof fersmite shares textural similarities with niobate mineral occurrences reported in 'alpine cleft' occurrences in Europe, and differs texturally and compositionally from fersmite in carbonatite-related Nb mineralization where it is considered secondary and derived from pre-existing niobate minerals. The Mount Brussilof fersmite probably precipitated from hydrothermal fluids. Fersmite has potential as a direct indicator mineral.

Acknowledgments

References cited

Aitken, J.D., 1971. Control of Lower Paleozoic Sedimentary Facies by the Kicking Horse Rim, Southern Rocky Mountains, Canada. Bulletin of Canadian Petroleum Geology, 19, 557-569.

Aitken, J.D., 1978. Revised models for depositional grand cycles, Cambrian of the southern Rocky Mountains, Canada. Bulletin of Canadian Petroleum Geology, 26, 515-542.

Aitken, J.D., 1989. Birth, Growth and Death of the Middle Cambrian Cathedral Lithosome, Southern Rocky Mountains; Bulletin of Canadian Petroleum Geology, 37, 316-333.

Aitken, J.D., and Mcllreath, L.A., 1984. The Cathedral Reef Escarpment, a Cambrian Great Wall with Humble Origins. Geoscience, 13, 17-19.

Aitken, J.D., and Mcllreath, L.A., 1990. Comment on "The Burgess Shale: Not in the Shadow of the Cathedral Escarpment". Geoscience Canada, 17, 111-115.

Al-Aasm, I., 2003. Origin and characterization of hydrothermal dolomite in the Western Canadian Sedimentary Basin. Journal of Geochemical Exploration, 78, 9-15.

Al-Aasm, I., Lonnee, J., and Clarke, J., 2000. Multiple fluid flow events and the formation of saddle dolomite: examples from Middle Devonian carbonates of the Western Canada Sedimentary Basin. Journal of Geochemical Exploration, 69, 11-15.

Alfonso, P., Oliva, J., Calvo, D., Parcerisa, D., and Garcia-Valles, M., 2015. Nb-Ta oxide minerals of alluvial placers from the Sunas Belt, Precambrian shield of Bolivia. In: Mineral Resources in a Sustainable World, 13th SGA Biennial Meeting 2015, proceedings, 2, pp. 667-670.

Anthony, J.W., Bideaux, R.A., Bladh, K.W., and Nichols, M.C., Eds., 2017. Handbook of Mineralogy, Mineralogical Society of America, Chantilly, VA 20151-1110, USA. <http://www.handbookofmineralogy.org/> Accessed November 2017.

Aurisicchio, C., De Vito, C., Ferrini, V., and Orlandi, P., 2001. Nb-Ta oxide minerals from miarolitic pegmatites of the Baveno pink granite, NW Italy. Mineralogical Magazine, 65, 509-522.

Chakhmouradian, A.R., Reguir, E.P., Kressall, R.D., Crozier, J., Pisiak, L.K., Sidhu, R., and Yang, P., 2015. Carbonatite-hosted niobium deposit at Aley, northern British Columbia (Canada): Mineralogy, geochemistry and petrogenesis. Ore Geology Reviews, 64, 642-666.

Chudy, T.C., 2013. The petrogenesis of th Ta-bearing Fir Carbonatite system, east-central British Columbia, Canada. PhD thesis, University of British Columbia, British Columbia, Canada, 553 p.

Ercit, T.S., 2005. Identification and alteration trends of granitic-pegmatite-hosted (Y,REE,U,Th)-(Nb,Ta,Ti) oxide minerals: a statistical approach. Canadian Mineralogist, 43, 1291-1303.

Foord, E.E., and Mrose, M.E., 1978. Rynersonite, $Ca(Ta,Nb)_2O_6$, a new mineral from San Diego County, California. American Mineralogist, 63, 709-714.

Fritz, W.H., 1990. Comment: In Defence of the Escarpment near the Burgess Shale Fossil Locality. Geoscience Canada, 17, 106-110.

Guastoni, A., Diella, V., and Pezzotta, F., 2008. Vigezzite and associated oxides of Nb-Ta from emerald-bearing pegmatites of the Vigezzo Valley, Western Alps, Italy. The Canadian Mineralogist, 46, 619-633.

Karup-Møller, S., Rose-Hansen, J., and Sørensen, H., 2010. Eudialyte decomposition minerals with new hitherto undescribed phases from the Ilímaussaq complex, South Greenland. Bulletin of the Geological Society of Denmark, 58, pp. 75-88.

Leach, D.L., Sangster, D.F., Kelley, K.D., Large, R.R., Garven, G., Allen, C.R., Gutzmer, J., and Walters, S.G., 2005. Sediment-hosted lead-zinc deposits: a global perspective. Society of Economic Geologists, Economic Geology One Hundredth Anniversary Volume 1905-2005, 561-607.

Leech, G.B., 1966. Kananaskis Lakes. Geological Survey of Canada, Open File map 634 scale 1:126,720.

Lumpkin, G.R., and Ewing, R.C., 1992. Geochemical alteration of pyrochlore group minerals: Microlite subgroup. American Mineralogist, 77, 179-188.

Mäder, U.K., 1987. The Aley Carbonatite complex, northern Rocky Mountains, British Columbia. In: Geological Fieldwork 1986, British Columbia Ministry of Energy, Mines and Petroleum Resources, British Columbia Geological Survey Paper 1987-1, pp. 283-288.

Mackay, D.A.R., and Simandl, G.J., 2014. Geology, market and supply chain of niobium and tantalum-a review. Mineralium Deposita, 49, p. 1025-1047.

Mackay, D.A.R., Simandl, G.J., Ma, W., Redfearn, M., and Gravel, J., 2016. Indicator mineral-based exploration for carbonatites and related specialty metal deposits-A QEMSCAN® orientation survey, British Columbia, Canada. Journal of Geochemical Exploration, 165, 159-173.

McClenaghan, M.B., 2005. Indicator mineral methods in mineral exploration. Geochemistry: Exploration, Environment, Analysis, 5, 233-245.

McDonough, W.F., and Sun, S.S., 1995. The composition of the Earth. Chemical geology, 120, 223-253.

McMechan, M.E., and Leech, G.B., 2011. Geology, Mount Assiniboine, British Columbia. Geological Survey of Canada, Canadian Geoscience Map 13, scale 1:50,000.

Mrad, C., 2016. Fluid compartmentalization of Devonian and Mississippian dolostones, Western Canada Sedimentary Basin; evidence from fracture mineralization. M.Sc. thesis, University of Windsor, Ontario, Canada, 114 p.

Nesbitt, B.E., and Prochaska, W., 1998. Solute chemistry of inclusion fluids from sparry dolomites and magnesites in Middle Cambrian carbonate rocks of the southern Canadian Rocky Mountains. Canadian Journal of Earth Sciences, 35, 546-555.

Niggli, P., Koenigsbergejr, J., and Parker, R.L., 1940. Die Mineralien der Schweizeralpen-2 Bände. Basel, Wepf & Co.

Paradis, S., and Simandl, G.J., 2017. Is there a genetic link between the SEDEX and MVT deposits of the Canadian Cordillera? In: Rogers, N., (Ed.), Targeted Geoscience Initiative, 2016 Report of Activities, Geological Survey of Canada, Open File 8199, pp. 107-113.

Paradis, S., and Simandl, G.J., 2018. Are there genetic links between carbonate-hosted barite-zinc-lead sulphide deposits and magnesite mineralization in southeast British Columbia? In: Rogers, N., (Ed.), Targeted Geoscience Initiative, 2016 Report of Activities, Geological Survey of Canada, Open File 8358, pp. 217-227.

Paradis, S., Hannigan, P., and Dewing, K., 2007. Mississippi Valley-type lead-zinc deposits. In: Goodfellow, W.D., (Ed.), Mineral Deposits of Canada: A Synthesis of Major Deposit-Types, District Metallogeny, the Evolution of Geological Provinces, and Exploration Methods, Geological Association of Canada, Mineral Deposits Division, Special Publication No. 5, pp. 185-203.

Paton, C., Hellstrom, J., Paul, B., Woodhead, J., and Hergt, J., 2011.

122

Geological Fieldwork 2018, British Columbia Ministry of Energy, Mines and Petroleum Resources, British Columbia Geological Survey Paper 2019-01

Iolite: freeware for the visualisation and processing of mass spectrometric data. Journal of Analytical Atomic Spectrometry, 26, 2508-2518.

Pouchou, J.L., and Pichoir, F., 1984. Un nouveau modèle de calcul pour la microanalyse quantitative par spectrométrie des rayons X. La Recherche Aérospatiale, 3, 167-192.

Prsek, J.,Majka, J., Uher, P., and Chudik, P., 2010. Niobium-tantalum minerals in the Skoddefjellet NYF granitic pegmatite, Svalbard Archipelago, Norway: Primary versus secondary assemblage. Neues Jahrbuch für Mineralogie-Abhandlungen, 187, 235-248.

Root, K.G., 2001. Devonian Antler fold and thrust belt and foreland basin development in the southern Canadian Cordillera: Implication for the Western Canadian Sedimentary Basin. Bulletin of Canadian Petroleum Geology, 49, 7-36.

Rosenberg., P.E., Burt, D.M., and Holland, H.D., 1967. Calcite - dolomite - magnesite stability relations in solutions: The effect of ionic strength. Geochimica et Cosmochimica Acta, 31, 39l-396.

Simandl, G.J., and Hancock, K.D., 1991. Geology of the Mount Brussilof magnesite deposit, SE British Columbia. In: Geological Fieldwork 1990, British Columbia Ministry of Energy, Mines and Petroleum Resources, British Columbia Geological Survey Paper 1991-1, pp. 269-278.

Simandl, G.J., and Hancock, K.D., 1998. Sparry Magnesite. In: Geological Fieldwork 1997, British Columbia Ministry of Employment and Investment, Geological Survey Paper 1998-1, pp. 24E-1-24E-3.

Simandl, G.J., and Paradis, S., 2018. Carbonatites: related ore deposits, resources, footprint, and exploration methods. Applied Earth Science, 127, 123-152.

Simandl, G.J., Hancock, K.D., Hora, D.Z., and MacLean, M.E., 1992. Regional geology of the Mount Brussilof carbonate-hosted magnesite deposit, southeastern British Columbia, Canada. In: Hora, Z.D., Hamilton, W.N., Grant, B., and Kelly, P.D. (Eds.), Industrial Minerals of Alberta and British Columbia, Canada, proceedings of the 27th Forum on the Geology of Industrial Minerals, May 5-10, 1991, British Columbia Geological Survey Open File 1991-23 and Alberta Geological Survey Information Series 115, pp. 57-65.

Simandl, G.J., Jones, P.C., and Rotella M., 2002. Blue River Carbonatites, British Columbia-Primary Exploration Targets for Tantalum. In: Exploration and Mining in British Columbia 2001, pp. 73-82.

Simandl, G.J., Mackay, D.A.R., Ma, X., Luck, P., Gravel, J., and Akam, C., 2017. The direct indicator mineral concept and QEMSCAN® applied to exploration for carbonatite and carbonatite-related ore deposits. In: Ferbey, T., Plouffe, A., and Hickin, A.S., (Eds.), Indicator Minerals in Till and Stream Sediments of the Canadian Cordillera. Geological Association of Canada Special Paper Volume 50, and Mineralogical Association of Canada Topics in Mineral Sciences Volume 47, pp. 175-190.

Simandl, G.J., Burt, R.O., Trueman, D.L., and Paradis, S., 2018. Tantalum and Niobium: Deposits, resources, exploration methods, and market-primer for geoscientists. Geoscience Canada, vol. 45, p. 85-96. https://journals.lib.unb.ca/index.php/GC/article/view/26003/1882519204.

Škoda, R., and Novák, M., 2007. Y,REE,Nb,Ta,Ti-oxide (AB_2O_6) minerals from REL-REE euxenite-subtype pegmatites of the Třebíč Pluton, Czech Republic; substitutions and fractionation trends. Lithos, 95, 43-57.

Sweetapple, M.T., and Lumpkin, G.R., 2011. Secondary Ta-Nb oxide minerals of the Archaean Wodgina Pegmatite district, Western Australia, and their significance. Asociación Geológica Argentina, Serie D, Publicación Especial No. 14, 209-212.

Symons, D.T.A., Enkin, R.J., and Cioppa, M.T., 1999. Paleomagnetism in the Western Canada Sedimentary Basin: dating fluid flow and deformation events. Bulletin of Canadian Petroleum Geology, 47, 534-547.

Timofeev, A., Migdisov, A.A., and Williams-Jones, A.E., 2015. An experimental study of the solubility and speciation of niobium in fluoride-bearing aqueous solutions at elevated temperature. Geochimica et Cosmochimica Acta, 158, 103-111.

Timofeev, A., Migdisov, A.A., and Williams-Jones, A.E., 2017. An experimental study of the solubility and speciation of tantalum in fluoride-bearing aqueous solutions at elevated temperature. Geochimica et Cosmochimica Acta, 197, 294-304.

Uher, P., Cerny, P., and Chapman, R., 1998. Evolution of Nb,Ta-oxide minerals in the Prasiva granitic pegmatites, Slovakia. II. External hydrothermal Pb, Sb overprint. Canadian Mineralogist, 36, 535-545.

Yao, Q.J., and Demicco, R.V., 1995. Paleoflow patterns of dolomitizing fluids and paleo hydrogeology of the southern Canadian Rocky Mountains: evidence from dolomite geometry and numerical modeling. Geology, 23, 791-794.

Yao, Q.J, and Demicco, R.V., 1997. Dolomitization of the Cambrian carbonate platform, Southern Canadian Rocky Mountains: Dolomite front geometry, fluid inclusion geochemistry, isotopic signature, and hydrologic modelling studies. American Journal of Science, 297, 892-938.

123

Geological Fieldwork 2018, British Columbia Ministry of Energy, Mines and Petroleum Resources, British Columbia Geological Survey Paper 2019-01